

Electric dipole strength of ^{52}Ca

Y. TOGANO⁽¹⁾⁽²⁾, T. NAKAMURA⁽³⁾, T. KOBAYASHI⁽⁴⁾, T. AUMANN⁽⁵⁾⁽⁶⁾,
H. BABA⁽¹⁾, K. BORETZKY⁽⁶⁾, A. BRACCO⁽⁷⁾⁽⁸⁾, F. BROWNE⁽¹⁾, F. CAMERA⁽⁷⁾⁽⁸⁾,
H. CHAE⁽⁹⁾, S. CHAN⁽¹⁾, N. CHIGA⁽¹⁾, H. CHOI⁽⁹⁾, L. CORTÉS⁽¹⁾, F. DELAUNAY⁽¹⁰⁾,
D. DELL'AQUILA⁽¹¹⁾, Z. ELEKES⁽¹²⁾, Y. FUJINO⁽²⁾, I. GAŠPARIĆ⁽¹³⁾, J. GIBELIN⁽¹⁰⁾,
K. I. HAHN⁽¹⁴⁾, Z. HALASZ⁽¹²⁾, A. HORVAT⁽⁵⁾, K. IEKI⁽²⁾, T. INAKURA⁽³⁾,
T. ISOBE⁽¹⁾, D. KIM⁽¹⁴⁾, G. KIM⁽¹⁴⁾, H. KO⁽⁹⁾, Y. KONDO⁽³⁾, D. KÖRPER⁽⁶⁾,
S. KOYAMA⁽¹⁵⁾, Y. KUBOTA⁽¹⁾, I. KUTI⁽¹²⁾, M. MATSUMOTO⁽³⁾, A. MATTA⁽¹⁰⁾,
B. MILLION⁽⁷⁾, T. MOTOBAYASHI⁽¹⁾, I. MURRAY⁽¹⁾, N. NAKATSUKA⁽¹⁶⁾⁽¹⁾,
N. ORR⁽¹⁰⁾, H. OTSU⁽¹⁾, V. PANIN⁽¹⁾, S. Y. PARK⁽¹⁴⁾, W. RODRIGUEZ⁽¹⁷⁾,
D. ROSSI⁽⁵⁾, A. T. SAITO⁽³⁾, M. SASANO⁽¹⁾, H. SATO⁽¹⁾, Y. SHIMIZU⁽¹⁾,
H. SIMON⁽⁶⁾, L. STUHL⁽¹⁸⁾, Y. L. SUN⁽⁵⁾, S. TAKEUCHI⁽³⁾, T. TOMAI⁽³⁾,
H. TÖRNQVIST⁽⁶⁾, T. UESAKA⁽¹⁾, V. VAQUERO⁽¹⁹⁾, O. WIELAND⁽⁸⁾, K. WIMMER⁽¹⁵⁾,
H. YAMADA⁽³⁾, Z. YANG⁽¹⁾, M. YASUDA⁽³⁾ and K. YONEDA⁽¹⁾

⁽¹⁾ *RIKEN Nishina Center - Saitama 351-0198, Japan*

⁽²⁾ *Department of Physics, Rikkyo University - Tokyo 171-8501, Japan*

⁽³⁾ *Department of Physics, Tokyo Institute of Technology - Tokyo 152-8551, Japan*

⁽⁴⁾ *Department of Physics, Tohoku University - Miyagi 980-8578, Japan*

⁽⁵⁾ *Institut für Kernphysik, Technische Universität Darmstadt - D-64289 Darmstadt, Germany*

⁽⁶⁾ *GSI Helmholtzzentrum für Schwerionenforschung - 64291 Darmstadt, Germany*

⁽⁷⁾ *Dipartimento di Fisica dell'Università degli Studi di Milano - I-20133 Milano, Italy*

⁽⁸⁾ *INFN Sezione di Milano - I-20133 Milano, Italy*

⁽⁹⁾ *Department of Physics and Astronomy, Seoul National University - 599 Gwanak, Seoul 151-742, Republic of Korea*

⁽¹⁰⁾ *LPC Caen, ENSICAEN, Université de Caen, CNRS/IN2P3 - 14050 Caen Cedex, France*

⁽¹¹⁾ *Institut de Physique Nucléaire - 91406 Orsay, France*

⁽¹²⁾ *ATOMKI Debrecen - Bem tér 18/c, 4026 Debrecen, Hungary*

⁽¹³⁾ *Ruđer Bošković Institute - Bijenička cesta 54, 10000 Zagreb, Croatia*

⁽¹⁴⁾ *Department of Science Education and Department of Physics, Ewha Womans University Seoul 03760, Republic of Korea*

⁽¹⁵⁾ *Department of Physics, The University of Tokyo - Tokyo 113-0033, Japan*

⁽¹⁶⁾ *Department of Physics, Kyoto University - Kyoto 606-8502, Japan*

⁽¹⁷⁾ *Universidad Nacional de Colombia, Sede Bogotá, Facultad de Ciencias, Departamento de Física - Bogotá, 111321, Colombia*

⁽¹⁸⁾ *Center for Nuclear Study, The University of Tokyo - Tokyo 113-0033, Japan*

⁽¹⁹⁾ *Instituto de Estructura de la Materia, CSIC - E-28006 Madrid, Spain*

received 31 October 2023

Summary. — The electric dipole strength above the one-neutron separation energy has been measured in the neutron-rich nucleus ^{52}Ca using the Coulomb excitation at 223 MeV/nucleon in inverse kinematics. The γ -ray detector array CATANA, the neutron detector NeuLAND demonstrator, and the SAMURAI spectrometer at RIKEN Nishina Center were combined to reconstruct the excitation energy of ^{52}Ca . A observed sharp peak at the very low neutron energy in the $^{52}\text{Ca} \rightarrow ^{51}\text{Ca} + n$ channel indicates that ^{52}Ca has a sizable amount of dipole strength just above the one neutron threshold.

1. – Introduction

The equation of state (EOS) for neutron-rich matter holds significant importance in comprehending the bulk properties of neutron-rich nuclei and neutron stars. The neutron-skin thickness of these nuclei exhibits a notable correlation with the symmetry energy, which constitutes the isospin-asymmetric component of the EOS, especially in proximity to the saturation density [1]. Recent observations involving the gravitational waves and the electromagnetic counter part resulting from the binary neutron star merger [2,3] have intensified research interest in both the symmetry energy and the neutron-skin thickness.

The electric dipole polarizability (α_D), representing the inversely energy-weighted sum of dipole strength, offers a means to constrain the neutron-skin thickness [4,5]. Due to its substantial contribution to α_D , the low-lying dipole strength, often referred to as the pygmy dipole resonance (PDR), is of importance. The PDR is located around the one-neutron separation energy S_n , and its strength also holds potential for constraining the neutron-skin thickness [6,7].

Recent theoretical calculations have revealed a rapid increase in the PDR strength as the neutron number (N) rises within the range of $15 < N \leq 16$, $28 < N \leq 34$, and $50 < N \leq 56$ [8]. These calculations suggest the existence of a possible shell effect on the PDR, given that these neutron numbers correspond to the region where valence neutrons enter shells with low angular momentum. Furthermore, it is noteworthy that nuclei featuring these specific neutron numbers exhibit a stronger correlation with the neutron-skin thickness when compared to other nuclei [9]. Building upon these theoretical studies, we conducted experimental investigations into the electric dipole strengths of ^{50}Ca and ^{52}Ca , both possessing neutron numbers of 30 and 32, in order to explore the neutron number dependence of the PDR and neutron-skin thickness. In this context, we present here preliminary results concerning ^{52}Ca .

2. – Experiment

The experiment was conducted at the RI Beam Factory (RIBF) located at RIKEN. The production of the ^{52}Ca beam was accomplished through the projectile fragmentation of a 345 MeV/nucleon ^{70}Zn beam, which was directed onto a 10-mm thick ^9Be target. Subsequent separation of the ^{52}Ca beam was achieved using the BigRIPS separator [10]. This ^{52}Ca beam was then transported to the SAMURAI spectrometer and impinged on

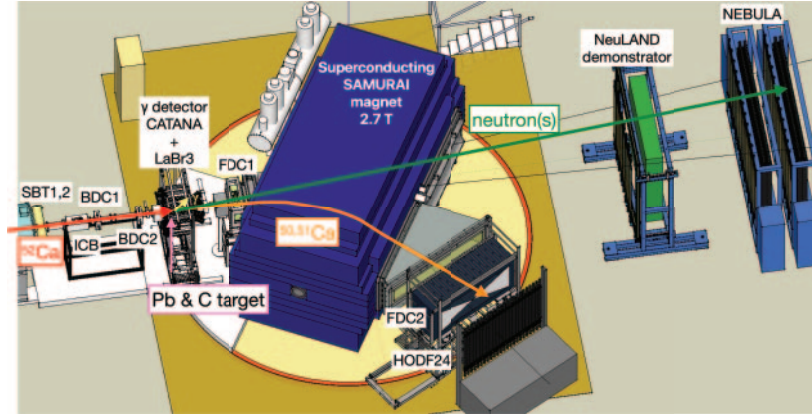


Fig. 1. – A schematic view of the experimental setup.

a Pb target for the Coulomb excitation. A complementary measurement was carried out using a C target to assess the contribution from nuclear excitations. The energy of ^{52}Ca at the center of the target was 223 MeV/nucleon.

To reconstruct the excitation energy above the one-neutron threshold in ^{52}Ca , the momenta of all reaction residues, including γ -rays, were determined through the experimental setup employing the SAMURAI spectrometer [11, 12], as depicted in fig. 1. The identification of the incoming beams was performed through the integration of several observables, including the beam momentum reconstructed in the BigRIPS, time-of-flight measurements utilizing plastic scintillators in the BigRIPS, SBT1 and SBT2, as well as ΔE obtained from the ionization chamber ICB. The incident angle and position upon the targets were monitored by two drift chambers, BDC1 and BDC2.

The momenta of de-excitation γ -rays from reaction residues were measured using the γ -ray detector array CATANA [13], along with 8 $\text{LaBr}_3\text{:Ce}$ detectors [14]. The CATANA array comprises 100 $\text{CsI}(\text{Na})$ scintillators, each with a thickness ranging from 90 to 120 mm, arranged in proximity to the targets. The isotopic identification and momentum reconstruction of charged residues were carried out with the aid of drift chambers, FDC1 and FDC2, positioned at the entrance and exit of the superconducting SAMURAI magnet. Furthermore, a hodoscope was incorporated, consisting of 24 plastic scintillator bars, located at the downstream of FDC2. This setup allowed for a reliable separation of the charge and mass of the charged residue, achieving 6σ and 7σ separation, respectively. Lastly, the momenta of neutrons originating from the reaction were determined through a combination of two neutron detectors, the NeuLAND demonstrator [15] and the NEBULA [16], both located downstream of the magnet.

3. – Results

Figure 2 illustrates the neutron energy and γ -ray energy distributions in the projectile-rest frame for the one neutron decay channel of the $^{52}\text{Ca} + \text{Pb}$ reaction. The black circles shows the experimental data. The orange histograms are the best fit by the response functions of direct (red histograms) and statistical (green histograms) decays. The detail of the fitting and the response functions are described later. The neutron energy spectrum (fig. 2(a) exhibits a distinct peak at low energy, indicative of the presence of a resonance

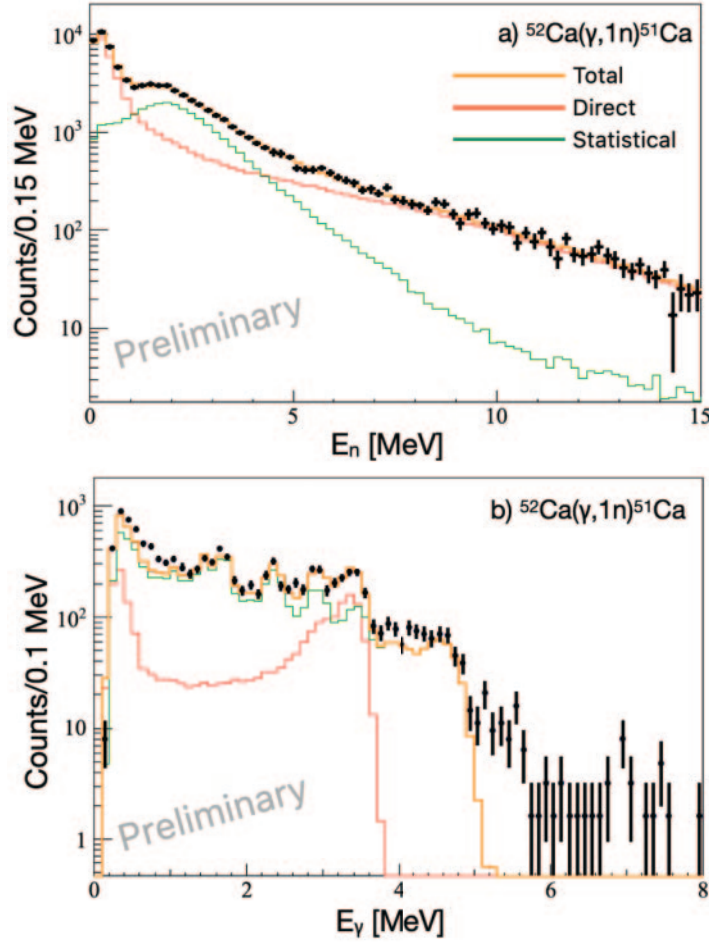


Fig. 2. – Neutron kinetic energy and γ -ray energy spectra in the projectile-rest frame for the 1 neutron-decay channel of $^{52}\text{Ca} + \text{Pb}$ reaction. a) Neutron kinetic energy of $^{52}\text{Ca} \rightarrow ^{51}\text{Ca} + n$ channel. b) γ -ray energies emitted from ^{51}Ca in 1 neutron-decay channel. The black circles are the experimental data, and the orange histograms correspond to the best fit by the direct (red) and statistical (green) components.

with a narrow width at low excitation energy. In the γ -ray energy spectrum (fig. 2(b)), multiple peaks are observed, corresponding to γ -rays from known excited states in ^{51}Ca . Notably, the appearance of a peak at 3.4 MeV in fig. 2(b) indicates the occurrence of direct decay through neutron hole states during the decay process of the ^{52}Ca excited states, as the 3.4 MeV state in ^{51}Ca is the $f_{7/2}$ neutron hole state of ^{52}Ca [19].

The direct decay to the 3.4 MeV state in ^{51}Ca can also be confirmed by examining the correlation between neutron energy and γ -ray energy, as presented in fig. 3. Figure 3 shows a two dimensional plot of the γ -ray energy and the neutron energy for the one-neutron decay channel. Neutron energies coinciding with the ~ 0.4 -MeV and 3.4-MeV γ -ray exhibit an extended tail towards higher energies, whereas neutrons coinciding with other γ rays are predominantly concentrated at lower neutron energies. Since the neutron

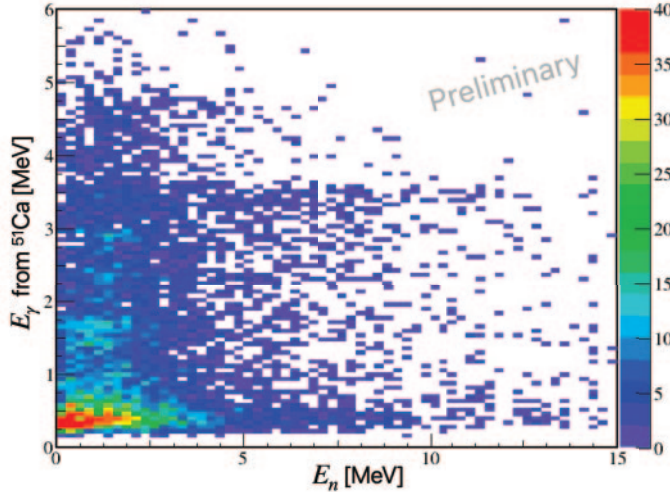


Fig. 3. – Correlation of γ -ray energy and the neutron energy for the 1 neutron decay channel. The z axis corresponds to the number of counts. The neutrons coincident with 3.4 MeV γ -ray have longer tail to the higher energies.

energy distribution resulting from statistical decay follows a Maxwell distribution peaking at a few MeV [20], the longer energy tail of neutrons coincident with the 3.4 MeV γ rays convincingly indicates that the 3.4 MeV state in ^{51}Ca is primarily populated through the direct decay of ^{52}Ca . The longer energy tail coincident with the ~ 0.4 -MeV γ rays is caused by the accidental coincidence between the γ ray background and the direct decay to the ^{51}Ca ground state or 3.4-MeV state, as intense X-rays from an atomic intereaction between the ^{52}Ca beams and the Pb target creates the background in γ -ray spectrum at energies less than 0.6 MeV. Additionally, the correlation in fig. 3 reveals that the sharp peak at very low neutron energy in fig. 2(a) does not coincide with any γ -rays above 0.6 MeV. It confirms that the excitation energy of the sharp peak is just above the neutron separation energy.

The excitation energy of ^{52}Ca can be determined as the sum of neutron energies and γ -ray energies; however, the detector response and inherent inefficiencies for both neutrons and γ -rays introduce distortions into these energy distributions. To accurately reconstruct the excitation energy of ^{52}Ca , taking into account these effects, we employed a simultaneous fitting approach that involved the measured distributions and the simulated detector response functions. This methodology resembles the one previously applied to extract the dipole strength of ^{68}Ni [17].

To reconstruct the excitation energy spectrum of ^{52}Ca , we performed a simultaneous fit, considering neutron energies, total neutron energy, γ -ray energies, and the combined sum of neutron and γ -ray energies of the one neutron decay channels. We employed a range of independent bins spanning from 6 to 20 MeV in excitation energy of ^{52}Ca as input for the fitting process. Response functions derived from Monte Carlo simulations based on GEANT4 for each energy bin were used as fitting functions. The simulated response encompasses both statistical and direct components of the decay of ^{52}Ca . The statistical decay component is computed using the nuclear reaction code TALYS [18]. The orange histograms in fig. 2 depict the best fit obtained by the direct (red) and

statistical (blue) decay components. The direct decay comprises two components: decay into the ^{51}Ca ground state and decay to the 3.4 MeV state in ^{51}Ca . The sharp peak in fig. 2(a) is well reproduced by the direct decay, underscoring the presence of a pronounced narrow dipole strength in ^{52}Ca close to the one-neutron threshold. The reconstruction of the electric dipole strength distribution of ^{52}Ca is ongoing.

4. – Summary

The measurement of electric dipole strength in ^{52}Ca , located above the one-neutron separation energy, was conducted through relativistic Coulomb excitation, employing a combination of the γ -ray detector array CATANA, the SAMURAI spectrometer, and the NeuLAND demonstrator. The energies of both neutrons and γ -rays arising from the 1 and 2 neutron decay channels of ^{52}Ca were obtained and will be utilized in the reconstruction of the excitation energy in ^{52}Ca . The evidence of the direct decay to a neutron hole state in ^{51}Ca was obtained from the correlation of the γ -rays and neutron energies. The observation of a distinct and sharp peak at low neutron energy in the one neutron decay channel serves as evidence that ^{52}Ca possesses a significant amount of dipole strength positioned just above the one-neutron threshold.

* * *

The authors thank the staffs of RIKEN RIBF and CNS for their efforts in providing the primary and secondary beams. The present work was supported in part by JSPS Grant-in-Aid for Scientific Research Grants No. JP21H01114, JSPS KAKENHI Grant No. 24105005.

REFERENCES

- [1] FATTOYEV F. J. and PIEKAREWIVZ J., *Phys. Rev. C*, **86** (2012) 015802.
- [2] ABBOTT B. P. *et al.*, *Astrophys. J.*, **848** (2017) L12.
- [3] ABBOTT B. P. *et al.*, *Phys. Rev. Lett.*, **120** (2017) 161101.
- [4] TAMII A. *et al.*, *Phys. Rev. Lett.*, **107** (2011) 062502.
- [5] TAMII A., VON NEUMANN-COSEL P. and POLTORATSKA I., *Eur. Phys. J. A*, **50** (2014) 28.
- [6] PIEKAREWICZ J., *Phys. Rev. C*, **73** (2006) 044325.
- [7] ROCA-MAZA X. and PARR N., *Prog. Part. Nucl. Phys.*, **101** (2018) 96.
- [8] INAKURA T., NAKATSUKASA T. and YABANA K., *Phys. Rev. C*, **84** (2011) 021302(R).
- [9] INAKURA T., NAKATSUKASA T. and YABANA K., *Phys. Rev. C*, **88** (2013) 051305(R).
- [10] KUBO T., *Nucl. Instrum. Methods Phys. Res. Sect. B*, **204** (2003) 97.
- [11] KOBAYASHI T., CHIGA N. *et al.*, *Nucl. Instrum. Methods Phys. Res. Sect. B*, **317** (2013) 294.
- [12] SHIMIZU Y., OTSU H. *et al.*, *Nucl. Instrum. Methods Phys. Res. Sect. B*, **317** (2013) 739.
- [13] TOGANO Y., NAKAMURA T. *et al.*, *Nucl. Instrum. Methods Phys. Res. Sect. B*, **463** (2020) 195.
- [14] GIAZ A., PELLEGRINI L. *et al.*, *Nucl. Instrum. Methods Phys. Res. Sect. A*, **729** (2013) 910.
- [15] BORETZKY K. *et al.*, *Nucl. Instrum. Methods Phys. Res. Sect. A*, **1014** (2021) 165701.
- [16] NAKAMURA T. and KONDO Y., *Nucl. Instrum. Methods Phys. Res. Sect. B*, **376** (2016) 156.
- [17] ROSSI D. M. *et al.*, *Phys. Rev. Lett.*, **111** (2013) 242503.
- [18] KONING A. J., HILAIRE S. and DUIJVESTIJN M. C., *Proceedings of the International Conference on Nuclear Data for Science and Technology*, edited by BERSILLON O., GUNSING F., BAUGE E., JACQMIN R. and LERAY S. (EDP Sciences) 2008, pp. 211–214.
- [19] ENCIU M. *et al.*, *Phys. Rev. Lett.*, **129** (2022) 262501.
- [20] BOHR A., MOTTELSON B. R., *Nuclear Structure*, Vol. **1** (W. A. Benjamin, New York).